

Curves-on-Surface: A General Shape Comparison Framework

Xin Li Ying He Xianfeng Gu Hong Qin
Stony Brook University, Stony Brook, NY 11794, USA
{xinli, yhe, gu, qin}@cs.sunysb.edu

Abstract

We develop a new surface matching framework to handle surface comparisons based on the mathematical analysis of curves on surfaces, and propose a unique signature for any closed curve on a surface. The signature describes not only the shape of the curve, but also the intrinsic relationship between the curve and its embedding surface; and furthermore, the signature metric is stable across surfaces sharing similar Riemannian geometry metrics. Based on this theoretical advance, we analyze and align features defined as closed curves on surfaces using their signatures. These curves segment a surface into different regions which are mapped onto canonical domains for the matching purpose. The experimental results are very promising, demonstrating that the curve signatures and the comparison framework are robust and discriminative for the effective shape comparison. Besides its utility in our current framework, we believe the curve signature will also serve as a powerful shape segmentation/mapping tool and can be used to aid in many existing techniques towards effective shape analysis.

1 Introduction

Shape comparison remains a central technical problem for effective 3D object search engine design. The technical challenge is how to devise an accurate and unique shape signature that can effectively distinguish one shape from the rest for analysis and retrieval. To date, a wide range of shape analysis techniques has been developed towards this goal especially during the last ten years. Examining the existing literatures, global properties (such as skeleton, size, and pose) are usually collected and analyzed, which gives rise to a quantitatively global difference for shape classification in an efficient and simple way. In contrast, matching techniques such as registration have been extensively developed for 2D/3D images comparison, especially in medical imaging and processing. The unique advantage for matching is that not only can we quantify the global difference but also we can accurately pinpoint all the local variations and calculate their distributions towards further analysis. Our objective is a shape matching and comparison method capturing both global differences and local variations.

Most of the current shape comparison techniques [14, 13, 5, 10, 12, 15, 18, 9, 2, 3, 4, 16, 1] are driven by comparing some collected global characteristics of the geometric objects. They try to compare the objects in a global sense,

relying exclusively on their geometric information without taking into account of the semantic feature curves. In this paper, we start our shape comparison task from a different perspective by considering all the closed curves on a surface.

1.1 Theoretic Foundation of Curve Space on Surface

We define the set of all closed curves on a surface M as *curve space* and denote it as $\Omega(M)$. The *curve space* on surfaces contains all the relevant geometric information of the surface and is easy to process. This philosophy on analyzing shapes via their associated curve space has a technically sound foundation in algebraic topology, infinite-dimensional Morse theory and Teichmüller space theory in complex geometry. Milnor[11] pointed out that $\Omega(M)$ is an infinite-dimensional manifold, the length of curves on a surface is a *Morse function*, and its critical points are *geodesics*. Morse theory is used to analyze the topology of $\Omega(M)$, which determines the topology of M . From the point of view of differential geometry, we know that the shape of the surface is locally determined by all the curves defined in the neighborhood. Motivated by the above results, our current research naturally follows the same methodology, and is specifically based on Teichmüller space theory.

Consider two surfaces M_1 and M_2 (Fig 1(a)), $\phi : M_1 \rightarrow M_2$ is a diffeomorphism between them, any curve (By curve, we mean closed curve in the remainder of this paper.) $\Gamma_1 \in \Omega(M_1)$ will be mapped to a curve in $\Omega(M_2)$ under this mapping: $\Gamma_2 = \phi \circ \Gamma_1$. Therefore, ϕ induces a one-to-one mapping ϕ^* from $\Omega(M_1)$ to $\Omega(M_2)$ by $\phi^* : \Omega(M_1) \rightarrow \Omega(M_2)$. The intrinsic relations between surfaces can be analyzed by studying ϕ^* instead of ϕ .

Furthermore, we map the curve space $\Omega(M)$ to a canonical Lie group $Diff(S^1)$, where $Diff(S^1)$ denotes the group of all diffeomorphisms from the unit circle S^1 to itself. We denote this map as $g_i : \Omega(M_i) \rightarrow Diff(S^1)$. Consequently, $\phi^* : \Omega(M_1) \rightarrow \Omega(M_2)$ induces a mapping from $Diff(S^1)$ to itself by $\bar{\phi} := g_2 \circ \phi^* \circ g_1^{-1}$.

The diagram in Fig 1(a) conveys our methodology in a graphical means: three mappings $\phi, \phi^*, \bar{\phi}$ are closely related; any one of them determines the remaining two. In other words, for the purpose of studying surfaces M_1, M_2 and the maps ϕ between them, we can study their curve space $\Omega(M_1), \Omega(M_2)$, signatures of the curves $Diff(S^1)$, and the mappings $\phi^*, \bar{\phi}$. We propose the following theoretic results to further re-enforce the above geometric intuition.

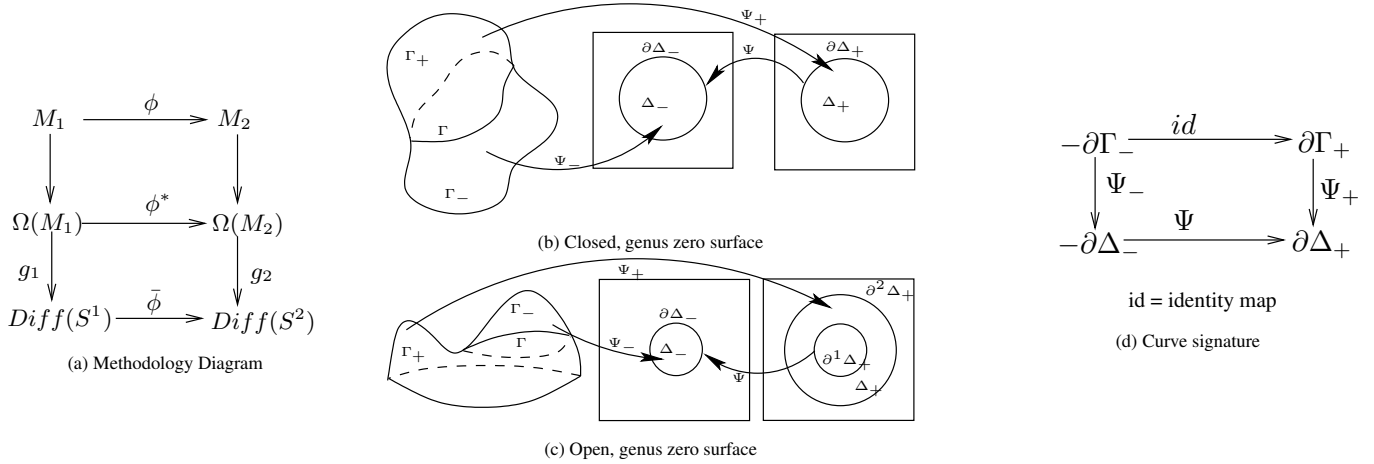


Figure 1. Theory foundation of curve signatures

Theorem 1 *If M is an oriented genus zero metric surface, then the curve space $\Omega(M)$ and $Diff(S^1)$ are equipped with L^2 metric, the map Ψ from its curve space $\Omega(M)$ to $Diff(S^1)$ is a homeomorphism.*

Therefore, in order to measure the distance between two curves on a surface, it is sufficient to measure the distance between two signatures defined in $Diff(S^1)$.

Theorem 2 *M_1 and M_2 are two oriented metric surfaces, ϕ is a conformal map if and only if $\bar{\phi}$ is the identity map of $Diff(S^1)$.*

The mapping from ϕ to $\bar{\phi}$, $F : \phi \rightarrow \bar{\phi}$ reveals a lot of geometric information about M_1 and M_2 . By choosing appropriate metrics, F is continuous. The kernel of F is all the conformal mappings between M_1 and M_2 .

2 Signatures in Curve Space

This section outlines our theoretical results on how to compute curve signatures for curves defined on a surface.

2.1 Theory and Algorithm Overview

Given a simple closed curve Γ on a genus zero surface M , the central idea for computing its signature is illustrated in Fig 1(b), (c), (d).

Case 1: If M is closed, as shown in Fig 1(b), then Γ partitions M into two components Γ_+ , Γ_- , both are topological disks and can be conformally mapped onto planar unit disks Δ_+ , Δ_- by Ψ_+ , Ψ_- . Γ is the boundary of Γ_+ and Γ_- , denoted by $\partial\Gamma_+ = \Gamma$ and $\partial\Gamma_- = -\Gamma$, and is mapped to the disk boundary, which are unit circles $\Delta = \partial\Delta_+ = -\partial\Delta_-$. The mapping induced by Ψ_+ and Ψ_- on the boundaries $\partial\Delta_+$ and $\partial\Delta_-$ is a diffeomorphism (differentiable and has a differentiable inverse). This diffeomorphism $\Psi : \partial\Delta_+ \rightarrow \partial\Delta_-$ is the *signature* of Γ .

Case 2: If M is open, as shown in Fig 1(c), then Γ partitions M into a topological disk Γ_- and a topological annulus Γ_+ . Γ_- can be conformally mapped onto a unit disk Δ_- , while Γ_+ can be conformally mapped onto an annulus Δ_+ with unit inner radius. We denote such annulus with unit inner radius as *canonical annulus*, the inner boundary of Δ_+

as $\partial^1\Delta_+$, and use the diffeomorphism $\Psi : \partial\Delta_- \rightarrow \partial^1\Delta_+$ as the signature of Γ .

In [17], Sharon and Mumford used Teichmüller theory to prove that any simple closed planar curve can be represented by such a diffeomorphism from a unit circle to itself uniquely up to scaling and translation. In this paper, we generalize this idea to arbitrary genus zero surfaces using Riemann surface theory.

In technical essence, we compute the conformal mapping for each component segmented by the curve, and take the boundary mappings Ψ as shown in Fig 1(d) as the signature. Some landmarks and constraints are used to eliminate the so-called Möbius ambiguity.

2.2 Conformal Map from an Open Genus-zero Surface to a Disk

We seek a conformal map Φ from a disk-like surface M to a unit disk. The map does exist according to Riemann mapping theory. Extensive relevant work has been done on finding a good *parameterization* for disk-like surfaces. However, complete conformality is usually not guaranteed. Based on the fact that the harmonic map from a closed genus zero surface to a sphere is also conformal, we use the *double covering* technique [8] to convert an open surface to a closed one, and reduce computing Φ to computing a harmonic map from *double covering* of M onto a sphere.

For an open surface M , we compute the double covering of M and then compute its harmonic mapping onto a sphere. Due to the exact symmetric property of double covering, the boundary ∂M is harmonically mapped onto the equator of the sphere and M is conformally mapped onto a hemisphere. Then we compose it with a stereographic projection to get a conformal map from M to the unit disk.

2.3 Conformal Map from a Closed Genus-zero Surface to a Sphere

To compute a conformal map Φ from a closed genus-zero surface M to a sphere, we initiate a map between them and minimize the harmonic energy by diffusing the heat-flow on

the sphere surface. This process is introduced and proved to converge to a harmonic/conformal map[7].

2.4 Conformal Map from a Topological Annulus to a Canonical Annulus

For curves on an open genus-zero surface, we need to compute a conformal map Φ from a topological annulus M (with $\partial M = \Gamma_1 - \Gamma_2$ where Γ_1 and Γ_2 are two boundaries) to a canonical planar annulus. First, we double-cover the surface to get a closed genus-one surface; next we compute a conformal map from a closed genus-one surface onto a rectangle planar domain by integrating a holomorphic 1-form [8] which describes two vector fields perpendicular to each other everywhere on surface; finally, we compose it with the conformal map from the rectangle to the canonical annulus using $e^{\frac{2\pi}{v}z}$ to get the ϕ .

2.5 Eliminating the Möbius Ambiguity

Conformal mappings between surfaces are not unique; e.g., all conformal mappings from a unit disk D^2 to itself form a Möbius group, with the form: $\tau : z \rightarrow w, w = e^{i\theta} \frac{z-z_0}{1-\bar{z}_0 z}, z, z_0 \in \mathbb{C}, \theta \in [0, 2\pi)$, where z_0 is a constant point, θ is a constant angle. All such τ form a 3 real dimensional group. Two mappings from a topological disk to a unit disk differ by a Möbius transformation. This ambiguity affects the signature and has to be eliminated via certain extra constraints.

For closed genus-zero surfaces, we first fix a marker point p on the surface and define a tangent direction \vec{t}_p going out from p . A closed curve Γ separates M into two disk-topology patches, the patch containing p is denoted as Γ_+ . We require that Ψ_+ maps p onto the origin, and \vec{t}_p onto the positive x-axis direction. These constraints uniquely determine Ψ_+ .

For open genus-zero surfaces, we fix the marker p on the boundary. Ψ_+ maps Γ_+ to Δ_+ , where Δ_+ is a canonical annulus with unit inner radius. The outer radius of Δ_+ is denoted as R , which is uniquely determined by the surface Γ_+ . Furthermore, we require that $\Psi_+(p) = (R, 0)$. Such Ψ_+ uniquely exists.

Through the above construction pipeline, every closed curve $\Gamma \in \Omega(M)$ corresponds to a diffeomorphism $\Psi \in Diff(S^1)$. Γ corresponds to two signatures Ψ_1, Ψ_2 if and only if there exists a Möbius transformation $\tau : D^2 \rightarrow D^2$, such that $\Psi_2 \circ \Psi_1^{-1} = \tau|_{\partial D^2}$. The above equation defines an equivalence relation \sim in $Diff(S^1)$. We claim that the mapping $\Psi : \Omega(M) \rightarrow Diff(S^1)/\sim$ is an one-to-one map. With appropriate metrics on $\Omega(M)$ and $Diff(S^1)$, it is a homeomorphism. In another word, each closed curve on M corresponds to an equivalence class of diffeomorphisms from the unit circle to itself.

In some scenarios, we might want to completely eliminate the ambiguity of signatures. For this purpose, we can further eliminate Möbius ambiguity using more markers. To uniquely reconstruct a curve, Ψ and three markers are sufficient for the closed genus-zero surfaces while for the open genus-zero surfaces, Ψ and two markers are sufficient.

2.6 Distances between Curves

For a genus-zero surface M , we create signatures for curves defined on M . The deviation between two curves can be measured by the distance between their signatures using *Weil-Peterson metric* on $Diff(S^1)$ as introduced in [17].

If surfaces M_1 and M_2 are sharing similar Riemannian metrics in \mathbb{R}^3 , then there exists a diffeomorphism $\phi : M_1 \rightarrow M_2$ close to an isometry, the induced map $\bar{\phi}$ between the signatures is close to the identity map from $Diff(S^1)$ to itself. In other words, if the curve $\Gamma_1 \subset M_1$ corresponds to $\Gamma_2 \subset M_2$ with $\Gamma_2 = \phi(\Gamma_1)$, then Γ_1 and Γ_2 have similar signatures. Hence, the signatures of curves have the property of strong stability under perturbation of Riemannian metric of their embedded surfaces and can be used to analyze curves on different surfaces as a robust tool.

Fig 3 demonstrates the stability of the signatures. All the curves and their corresponding signatures are drawn in the same color. Note that the signature is a diffeomorphism from a circle to itself, thus it can be considered as a periodic real function from $[0, 2\pi)$ to $[0, 2\pi)$ (only one period is shown in our figures). In (a), a planar rectangle is isometrically deformed to a cylinder, our computation shows that the corresponding curves have exactly the same signatures. In (b), the planar rectangle is perturbed about 6% in z direction, and about 1% in x, y directions, signatures of the corresponding curves are very close to each other. In (c), the planar surface (1) is simulated as cloth and is deformed as shown in (2), namely, it allows large bending but little stretching, the signatures of the corresponding curves are also almost identical (i.e., undistinguishable); also, the curve on surface (1) is perturbed slightly to the red curve in (3), the signature has little deviation.

Therefore, curves on different surfaces which are close to each other in terms of geometry (differ by a near-isometric mapping) can be robustly and accurately compared and analyzed using their signatures.

3 Surface Matching

Based on the analysis of curve space, we design our surface matching framework for curve alignment, surface registration, and shape comparison.

3.1 Feature Alignment for Surface Segmentation and Matching

Assume M_1 and M_2 are the two surfaces to be matched, if they share similar geometries, meaning there exists a mapping $\phi : M_1 \rightarrow M_2$ close to an isometry, then the following algorithm can be used for matching.

1. Extract feature curve set $\{\Gamma_1^1, \Gamma_2^1, \dots, \Gamma_n^1\}$ on M_1 . Such curves can be either marked by the user as certain meaningful features, or automatically computed based on geometric information of M_1 such as the extremals of the principal curvatures along the corresponding principal directions.
2. Compute the curve signatures of Γ_i^1 on M_1 and get the signature set $\{\Psi_1, \Psi_2, \dots, \Psi_n\}$.
3. Compute the curve set $\{\Gamma_1^2, \Gamma_2^2, \dots, \Gamma_n^2\}$ on M_2 , such that the curve signature of Γ_i^2 equals Ψ_i .

4. The curve set $\{\Gamma_i^k\}$ segments M_k to several connected components $\{c_1^k, c_2^k \dots, c_m^k\}$, $k = 1, 2$, such that the boundaries of c_i^1 correspond to the boundaries of c_i^2 . Match c_i^1 with c_i^2 pairwise on the planar domain.

If in the third step above, the user prefers to label the meaningful feature curve set on M_2 , we can change this step accordingly so that we compute, compare their signatures, and find the nearest one-to-one matching between these two sets of feature curves.

3.2 Surface Comparison in 2D Planar Canonical Domains

When all feature curves are matched, we segment the surfaces into several patches, each of which can be matched on the planar domain with many existing techniques. A possible technique is to use the *conformal representation*[6], which consists of two functions $\lambda(u, v), H(u, v)$ defined on canonical domains. λ is called *conformal factor*, representing the area stretching of the mapping from the original surface to the planar domain and H is the mean curvature implying the bending information of the surface. In our experiments, we normalize the original surface and then compute its conformal factor of each vertex by dividing its one-ring-neighbor area on the surface by its counterpart on the planar domain. The conformal representation is complete in the sense that it allows us to fully reconstruct the original surface from the representation[6]; also, it stably represents the geometry distance between surfaces in \mathbb{R}^3 ; the perturbation in geometry leads to a stable and continuous perturbation in their conformal representations; furthermore, as a by-product, the computation process of curve signatures has already got conformal maps from most 3D patches to the planar domains, so the surface matching based on these mappings can be done without further computation cost. The matching energy E between two corresponding surface patches M_0 and M_1 is defined on their common canonical planar domains D by $E = \int_{(u,v) \in D} \|\lambda_0(u, v) - \lambda_1(u, v)\|^2 dudv + \int_{(u,v) \in D} \|H_0(u, v) - H_1(u, v)\|^2 dudv$.

4 Experimental results

To illustrate our framework, we first present a human face matching example. Two human faces (f_0 (female) and f_1 (male) as shown in Fig 4 (a) and (b)) are compared by aligning feature curves enclosing eyes, noses and mouths. Assuming that the geometries of human faces are similar, namely, there exist mappings $\Phi : f_0 \rightarrow f_1$ that are close to isometry, we manually label on each face four feature curves and compute their signatures. The curves and their signatures are highlighted with the same color. For example, curves enclosing the right eyes and their signatures are colored in red. As shown in Fig 4 (c), signatures with the same color are quite similar to each other.

The experiment shows that similar feature curves on two faces have similar signatures, while different feature curves on the faces have apparently different signatures. Therefore, the curve signature is a reliable tool to align the same features

across different faces. The faces can then be segmented and mapped onto common canonical planar domains for subsequent registration and comparison, as shown in Fig 4 (d) and (e).

Another example is shown comparing a horse and its collapsed pose. Users first mark feature curves on one pose. With their signatures, we could reconstruct the curves on the second surface. Techniques introduced in [17] can be used to reconstruct the curve on the complex domain, which corresponds to a unique curve on the spherical domain. Combined with three predefined markers introduced in section 2.5 and the mapping from the original surface to the sphere, the unique curve on the original surface can be reconstructed. With this process, feature curves can be transferred onto the second object as shown in Fig 2. The original feature curves on the resting pose, their signatures, and the transferred curves are shown in the three rows in Fig 2 respectively.

The conformal factor and the mean curvature distributions of all parts are computed and color-coded in the first four rows of Fig 5 (the first two rows are for the standing pose, while the next two rows are for the collapsed pose).

The surface comparison framework can be interactively controlled by changing weights of the two terms in our matching energy. For example, if isometry-invariant comparison is preferred, only the stretching factor needs to be considered. So by ignoring the mean curvature, a metric invariant under bending is designed, which naturally leads to a bend-invariant or pose-invariant result. The conformal representation difference between the two horse models (a) and (b) is color-coded on the first model as shown in Fig 5 (c) and the difference ignoring the bending term is shown in Fig 5 (d); also, the difference with only the bending term is color-coded in (e). As shown in the above examples, our matching algorithm finds between two complicated objects a difference distribution which can be flexibly adjusted for different goals such as bending-invariant surface matching. Since it can catch the difference on the metric ignoring the embedding of the surface in \mathbb{R}^3 , it becomes a useful tool for non-rigid matching applications. One example is the colons matching and analysis in medical imaging. People with different poses under CT scans might have large bending differences on their colons with little changes in metric, in which case such a bending-invariant matching is ideal for analysis.

5 Conclusion and Future Work

We have designed a metric space for simple closed curves on genus-zero surfaces via conformal mappings. Curves on surfaces are represented by equivalence classes of diffeomorphisms of the unit circle to itself. The proposed curve signature corresponds uniquely to the curve defined on a surface. It also includes information of both the curve's shape and its embedding on the surface, which are invariant under isometry and stable under near-isometric transformation of surfaces, thus enables a powerful practical tool for the effective analysis of curves and surfaces among geometrically similar objects.

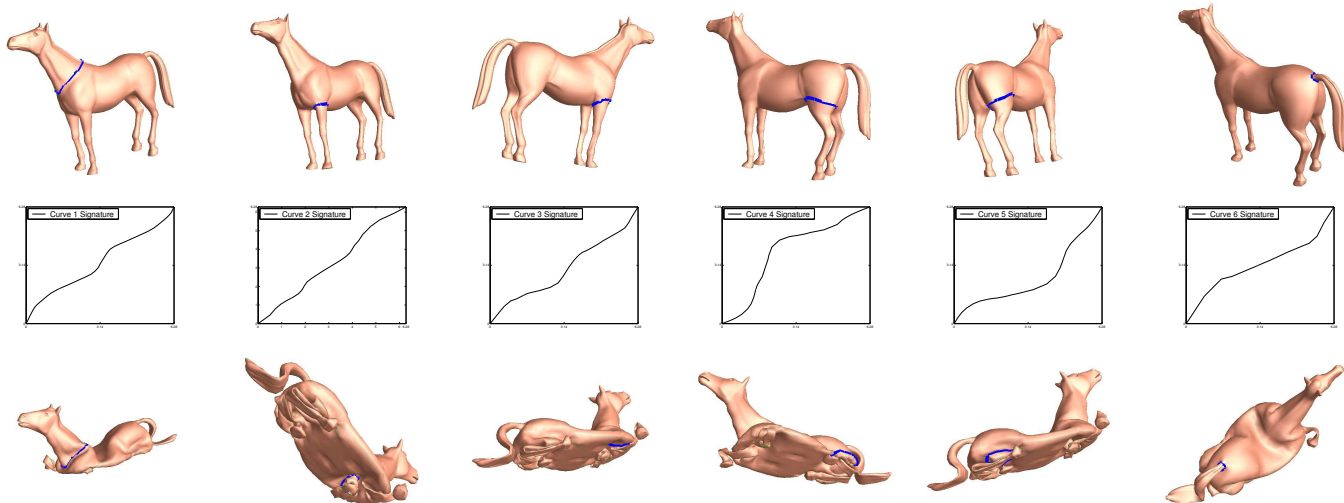


Figure 2. Row 1: feature curves on the standing-horse model. Row 2: the corresponding signatures. Row 3: the corresponding reconstructed curves on the collapsed-horse model.

Besides the above theoretical contributions, we develop a framework for shape registration and comparison guided by feature curves alignments. After curves with the most similar signatures are correctly identified and aligned, genus-zero surfaces are then segmented into several parts and registered separately. This automatic process accurately forces the alignment of feature curves and alleviates the difficulties of 3D surface matching by reducing it to the simple comparison of functions defined on canonical planar domains. Also, the algorithm can be flexibly adjusted to provide a pose-invariant shape descriptor.

One potential limitation is that the curve signature developed in this paper is perhaps best suitable to analyze curves defined on one surface or two surfaces of similar geometry. When the signature is compared for curves defined on different surfaces, it is only stable when there exists a near-isometric mapping between the surfaces. In general, aligning curves defined on surfaces with dramatically different geometry is technically challenging.

Constructing shape space of curves on surfaces with arbitrary topology is promising and challenging. We plan to explore further along these directions in the near future.

Acknowledgements

The research was supported in part by US National Science Foundation grants IIS-0082035 and IIS-0097646.

References

- [1] H. Alt, C. Knauer, and C. Wenk. Comparison of distance measures for planar curves. *Algorithmica*, 38(1):45–58, 2004.
- [2] S. Biasotti, S. Marini, M. Mortara, G. Patanè, M. Spagnuolo, and B. Falcidieno. 3D shape matching through topological structures. In *DGCI*, volume LNCS 2886, pages 194–203. Springer-Verlag, 2003.
- [3] T. K. Dey, J. Giesen, and S. Goswami. Shape segmentation and matching with flow discretization. In *WADS*, pages 25–36, 2003.
- [4] P. Donatini and P. Frosini. Natural pseudodistances between closed manifolds. *Forum Mathematicum*, 16(5):695–715, 2004.
- [5] R. Gal, A. Shamir, and D. Cohen-Or. Pose oblivious shape signature. 2005.
- [6] X. Gu and B. C. Vemuri. Matching 3d shapes using 2d conformal representations. In *MICCAI (1)*, pages 771–780, 2004.
- [7] X. Gu, Y. Wang, T. Chan, P. Thompson, and S.-T. Yau. Genus zero surface conformal mapping and its application to brain surface mapping. In *IPMI*, 2003.
- [8] X. Gu and S.-T. Yau. Surface classification using conformal structures. In *ICCV*, pages 701–708, 2003.
- [9] M. Hilaga, Y. Shinagawa, T. Kohmura, and T. L. Kunii. Topology matching for fully automatic similarity estimation of 3d shapes. In *SIGGRAPH*, pages 203–212, 2001.
- [10] M. Kazhdan and T. Funkhouser. Harmonic 3d shape matching. In *SIGGRAPH 2002 Technical Sketch*, 2002.
- [11] J. W. Milnor. *Morse Theory*. Princeton Univ. Press, 1963.
- [12] M. Novotni and R. Klein. 3d zernike descriptors for content based shape retrieval. In *SM*, pages 216–225, 2003.
- [13] R. Ohbuchi, T. Otagiri, M. Ibatto, and T. Takei. Shape-similarity search of three-dimensional models using parameterized statistics. In *PG*, pages 265–275, 2002.
- [14] R. Osada, T. A. Funkhouser, B. Chazelle, and D. P. Dobkin. Matching 3d models with shape distributions. In *SMI*, pages 154–166, 2001.
- [15] M. Reuter, F.-E. Wolter, and N. Peinecke. Laplace-spectra as fingerprints for shape matching. In *SPM*, pages 101–106, New York, NY, USA, 2005. ACM Press.
- [16] T. B. Sebastian, P. N. Klein, and B. B. Kimia. On aligning curves. *PAMI*, 25(1):116–125, 2003.
- [17] E. Sharon and D. Mumford. 2d-shape analysis using conformal mapping. In *CVPR (2)*, pages 350–357, 2004.
- [18] H. Sundar, D. Silver, N. Gagvani, and S. J. Dickinson. Skeleton based shape matching and retrieval. In *SMI*, pages 130–142, 290, 2003.

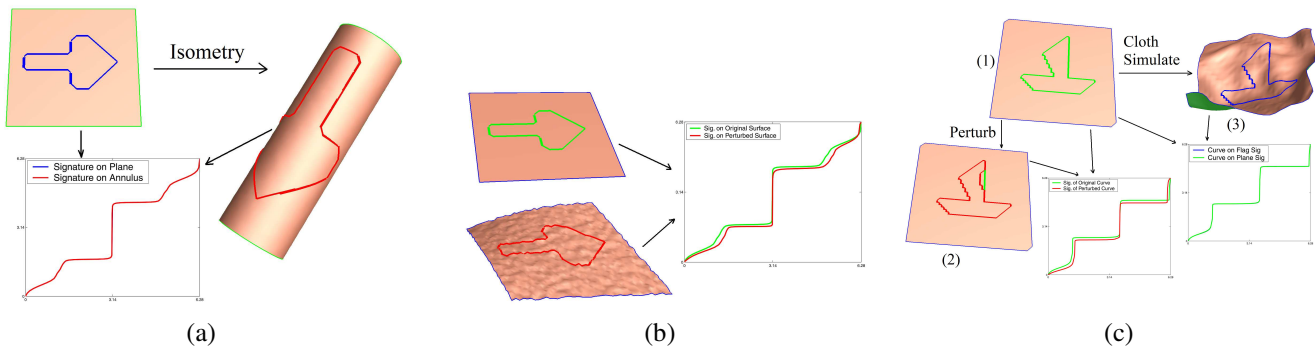


Figure 3. The stability of curve signatures under isometry, perturbation and bending of embedded surfaces.

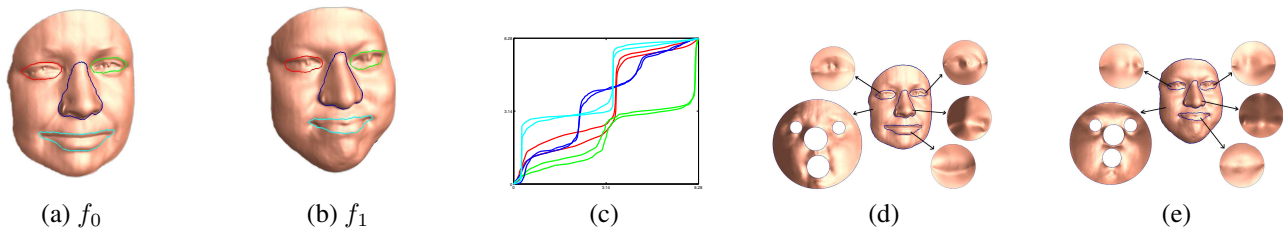


Figure 4. Curves on faces((a),(b)), their signatures(c), and the segmentations for the matching purpose((d),(e)).

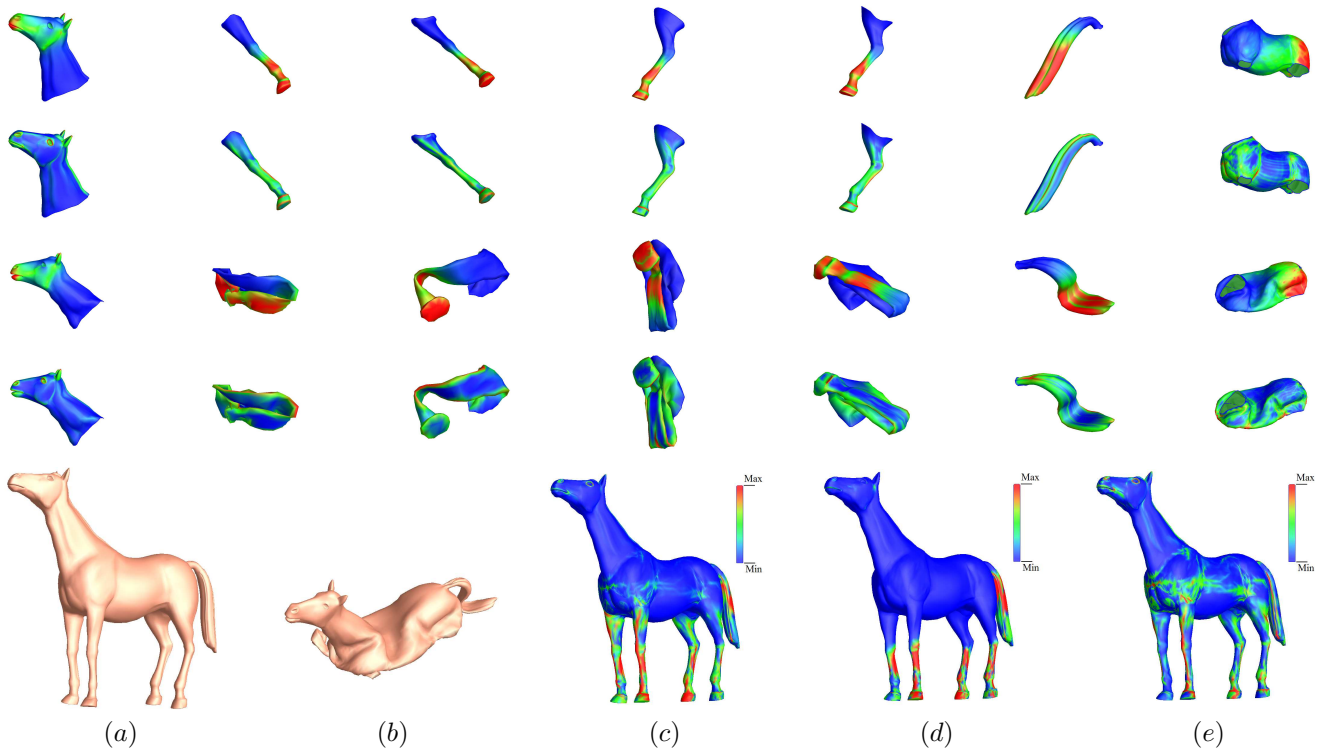


Figure 5. The first and the second rows show color-coded conformal factor λ and mean curvature H of the standing horse model; the third and fourth rows show λ and H of the collapsed horse model; the last row shows the final matching results between the standing model (a) and the collapsed model (b), with (c)-(e) color-coding differences on conformal representation, λ , and H respectively. (Mesh size: 17k triangles)